Department of Nuclear engineering
Nuclear Reactor Technology

PROJECT REPORT

ABWR - Team 21

Lecturers:
Pavel Kudinov

Students:
Diane Mauclère &
Paul Toris

Acedemic year of 2022/2023

Contents

1 Introduction

ABWR, which stands for Advanced Boiling Water Reactor, is a light water cooled reactor. It is one of the most advanced nuclear power plants in existence, offering numerous safety features and operational advantages over other reactor designs. The purpose of this project is to become familiar with the general features and operational principles of an ABWR, and to gain a better understanding of the design parameters of the reactor core.

This project will involve three tasks of literature studies, to gain an understanding of the general design specification of the ABWR, its operational principles, and its safety features. The last three tasks of the project will involve calculations to determine the basic design parameters of the reactor core, such as the axial pressure drop distribution, axial coolant enthalpy distribution, axial coolant temperature distribution, axial void fraction distribution, and the fuel temperature. With the completion of this project, the reader will have a comprehensive understanding of the ABWR and its core design parameters.

2 General design specification of the ABWR

The Advanced Boiling Water Reactor (ABWR) is a Generation III boiling water reactor (BWR) designed by General Electric (GE) and Toshiba. The ABWR's design draws heavily from the BWR-III design and combines the best features of previous BWR designs with advancements in materials, computer systems, and safety engineering (see figure 1). The ABWR can generate up to 1,350 MW of electricity, and is characterized by its high efficiency.

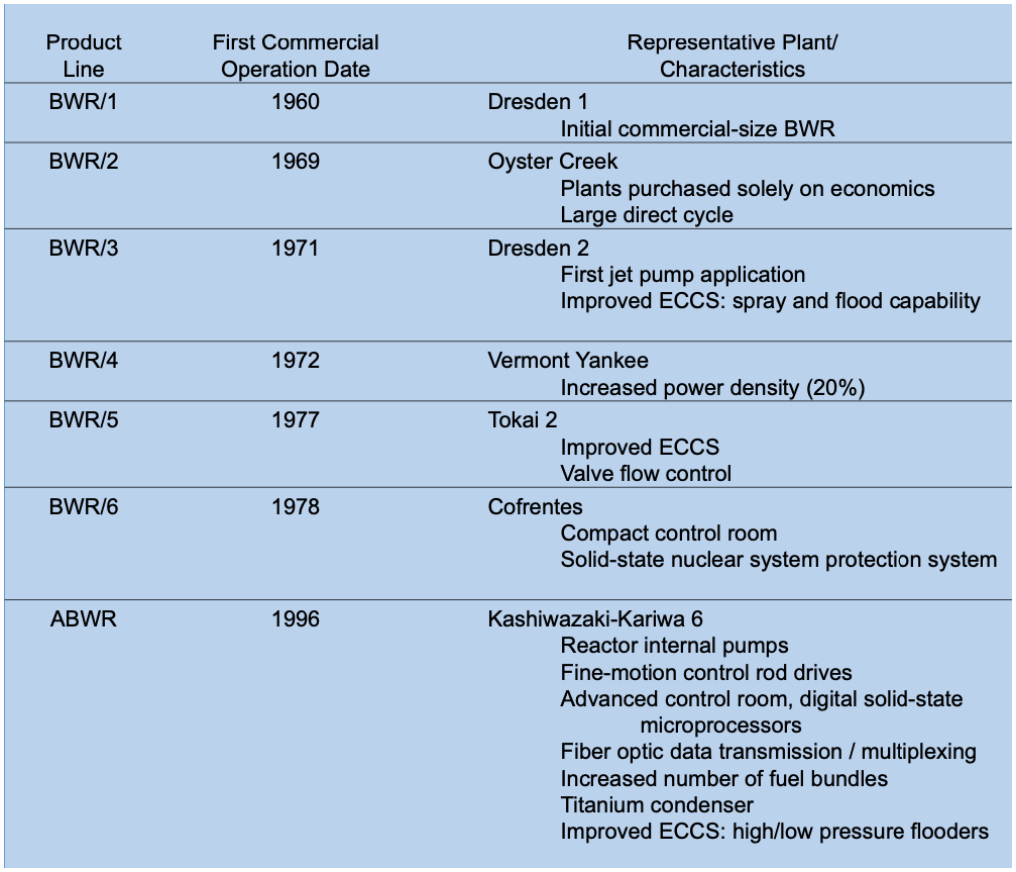

Product Line	First Commercial Operation Date	Representative Plant/ Characteristics
BWR/1	1960	Dresden 1 Initial commercial-size BWR
BWR/2	1969	Oyster Creek Plants purchased solely on economics Large direct cycle
BWR/3	1971	Dresden 2 First jet pump application Improved ECCS: spray and flood capability
BWR/4	1972	Vermont Yankee Increased power density (20%)
BWR/5	1977	Tokai 2 Improved ECCS Valve flow control
BWR/6	1978	Cofrentes Compact control room Solid-state nuclear system protection system
ABWR	1996	Kashiwazaki-Kariwa 6 Reactor internal pumps Fine-motion control rod drives Advanced control room, digital solid-state microprocessors Fiber optic data transmission / multiplexing Increased number of fuel bundles Titanium condenser Improved ECCS: high/low pressure flooders

Figure 1: Evolution of the GE BWR from [1].

As a boiling reactor, it is composed of a single loop circulation system. In this system, reactor coolant moves upwards through the core, absorbing heat as it goes, and producing a steam-water mixture. This mixture is then fed to two stages of moisture separation, where water droplets are removed. The resulting steam is directed to the steam line, which moves it to the main turbine, causing it to turn the turbine generator and produce electricity.

2.1 The reactor vessel

The vessel houses the reactor core, which contains fuel rods which create heat. Secondly, the reactor vessel serves as a barrier to contain the potentially harmful fission products that are produced during the reaction and protect from potential radiation exposure. Finally, the vessel provides the necessary volume for water to circulate and remove heat from the reactor core, keeping it cooled and moderating the neutrons. The figure 2 give a scheme of the ABWR vessel.

Compared to earlier product lines, the ABWR vessel has an increased diameter and decreased height, which has resulted in a thicker wall. Specifically, it has a height of approximately 21 m and a diameter of 7.4 m for this size of reactor.

The most significant change in the design of the ABWR is the elimination of the external loops and the incorporation of internal pumps for reactor coolant recirculation. The designs of the reactor pressure vessel and the core internals have been optimized for the internal pump concept. The pumps to circulate the reactor coolant are directly mounted to the bottom of the ABWR reactor pressure vessel. This system is simple because no external recirculation piping or jet pump is required. The elimination of the external recirculation piping is particularly significant, as it provides a wider space inside the primary containment vessel and removes a potential radiation source. As a result, work efficiency is enhanced and radiation exposure during maintenance work is reduced. Furthermore, because there

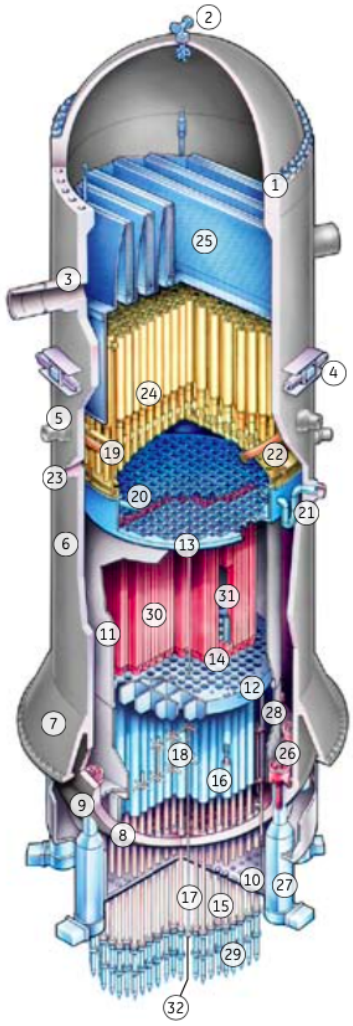

1 - Vessel flange and closure head
2 - Vent and head spray assembly
3 - Steam outlet flow restrictor
4 - RPV stabilizer
5 - Feedwater nozzle
6 - Forged shell rings
7 - Vessel support skirt
8 - Vessel bottom head
9 - RIP penetrations
10 - Thermal insulation
11 - Core shroud
12 - Core plate
13 - Top guide
14 - Fuel supports
15 - Control rod drive housings
16 - Control rod guide tubes
17 - In-core housing
18 - In-core guide tubes and stabilizers
19 - Feedwater sparger
20 - High pressure core flooder (HPCF) sparger
21 - HPCF coupling
22 - Low pressure flooder (LPFL)
23 - Shutdown cooling outlet
24 - Shroud head and steam separator assembly
25 - Steam dryer assembly
26 - Reactor internal pumps (RIP)
27 - RIP motor casing
28 - Core and RIP differential pressure line
29 - Fine motion control rod drives
30 - Fuel assemblies
31 - Control rods
32 - Local power range monitor

Figure 2: Scheme of the ABWR vessel from [1]

is no large-diameter nozzle below the core region of the reactor pressure vessel, there is no possibility of exposing fuel assemblies even in the case of LOCA, and thus safety is enhanced. These internal pumps have a smaller rotating inertia and, coupled with the solid-state variable frequency power supply, can respond quickly to grid load transients and operator demand [2]

2.2 The reactor Core and Fuel

In the ABWR, the reactor core is cylindrical and positioned upright, containing 872 fuel assemblies within the reactor vessel. Coolant flows upward through the core, and its arrangement of the quarter of the care and lattice configuration are shown in figure 3 and 4, respectively. The whole core configuration is deduced by symmetry. To decrease neutron leakage and facilitate control rod movement near low power fuel, fuel assemblies with low reactivity are positioned at the core periphery and in the control cells, respectively.

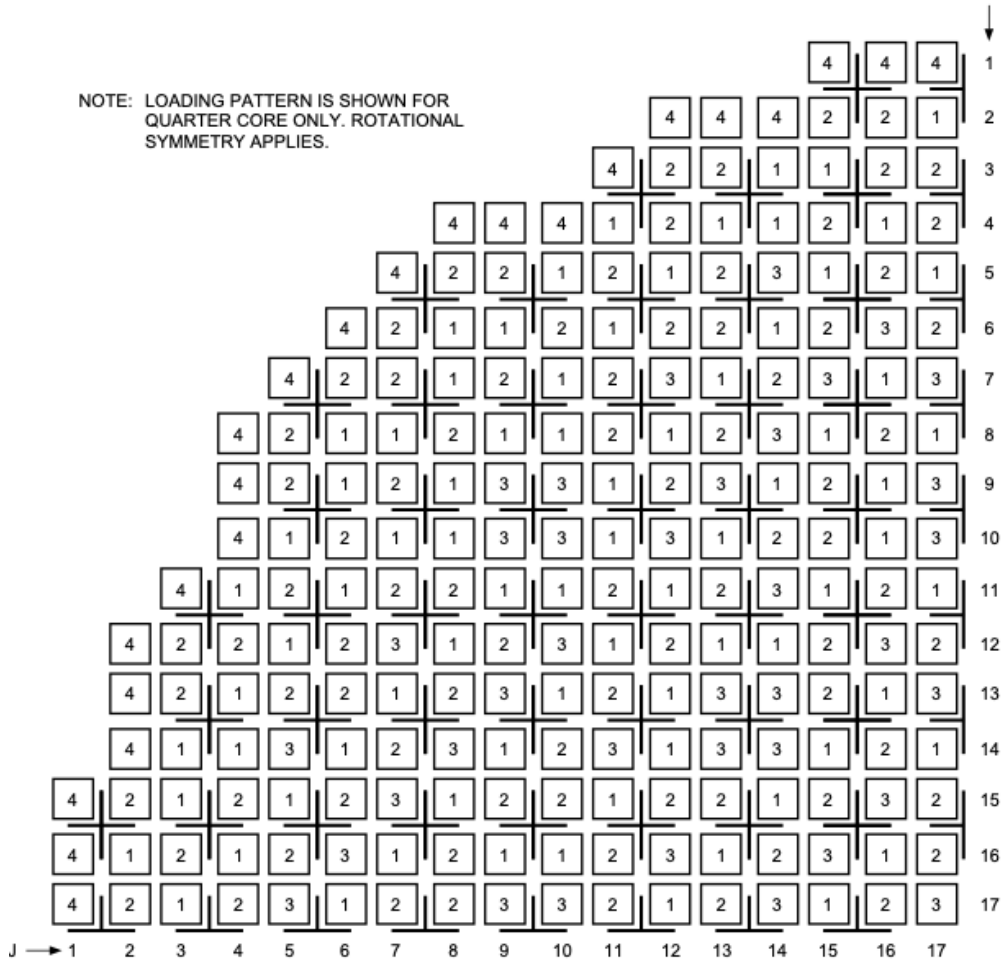

Figure 3: ABWR quarter core configuration from [3]

The fuel assembly consists of a fuel bundle and channel, with the former containing fuel rods and hardware to maintain their proper spacing, and the latter serving as a Zircaloy box to direct coolant flow and guide movable control rods. The fuel assemblies and control

rods of the ABWR follow the GE14 design which is used in most GE boiling water reactors. The GE14 design is currently the most advanced fuel assembly design from GE, consisting of a 10x10 array of 78 full length fuel rods, 14 part length rods, and two central water rods. Figure 5 shows the major components of the GE14 design, including the cast stainless steel lower and upper tie plates that maintain fuel rod spacing and facilitate lifting the bundle, respectively.

Additionally, eight tie rods and Zircaloy ferrule spacers along the length of the fuel bundle maintain proper rod spacing, prevent flow-induced vibration, and improve critical power performance.

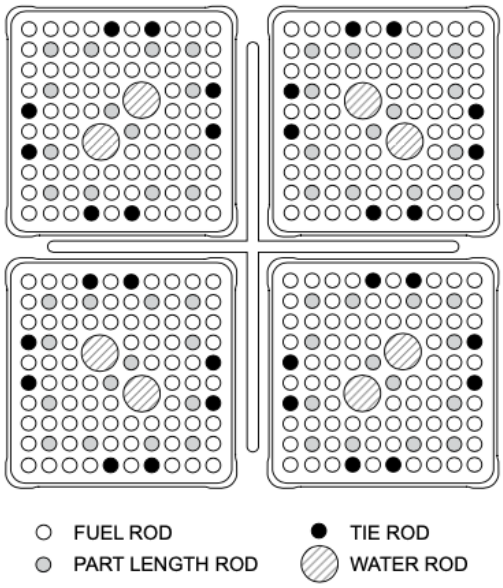

Figure 4: Four Bundle Fuel Modules from [1]

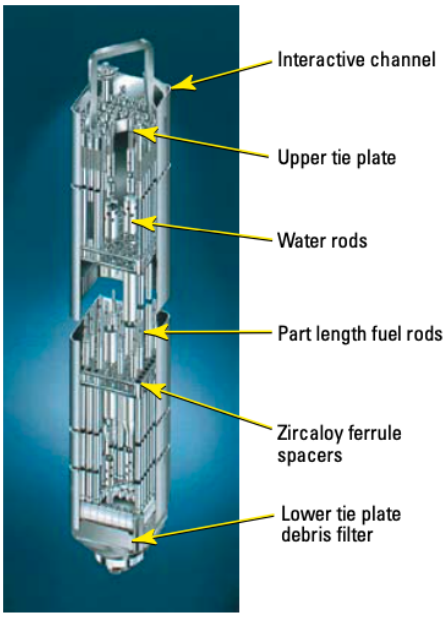

Figure 5: GE14 Fuel Assembly from [1]

2.3 Reactor containment

Initially, the first BWR containment structures were spherical ”dry” designs, similar to the ones still used in PWR designs today. However, the BWR quickly transitioned to the ”pressure suppression” containment design for several benefits, superior ability to handle rapid depressurization, unique capacity to filter and retain fission products, provision of readily available makeup water in case of accidents, and simplified, compact design.

The first of these new containment designs was the Mark I, which had a characteristic light bulb configuration. The conical Mark II design had a simpler arrangement based on steel-lined reinforced concrete, with a large containment drywell providing more room for steam and emergency core cooling systems piping. The Mark III design, used worldwide with BWR/6s and some BWR/5s, represented a significant improvement in simplicity. The ABWR containment is notably smaller than the Mark III containment due to the elimination of recirculation loops, resulting in a more compact containment and reactor building made of reinforced concrete with a steel liner. The evolution of the BWR containment design from the earliest versions to the ABWR design is illustrated in Figure 6, with the containment outlined in red when the reactor building is also depicted.

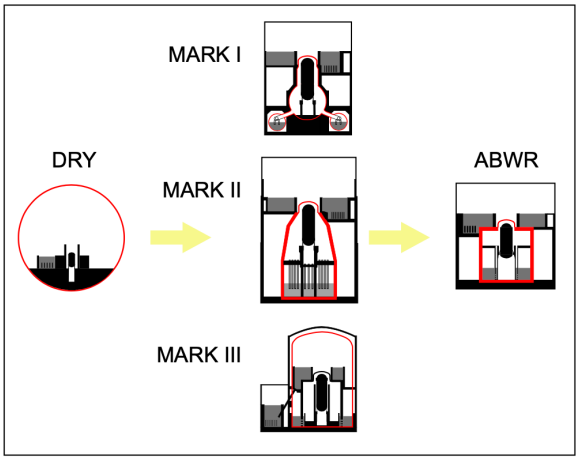

Figure 6: Evolution of BWR containment from [3]

2.4 Balance-Of-Plant Systems

The ABWR plant has a rated thermal output of 3926 MW and an electrical output of more than 1350 MWe. The turbine design includes a 52-in. last stage bucket design to improve plant efficiency, performance, and economy. The steam is reheated in two stages using combined moisture separator/reheaters to remove moisture. The new design also incorporates the concept of both high-pressure and low-pressure pumped-up drains to increase plant output and reduce cost. Instead of cascading the heater drains back to the condenser, the pumped-up drain system injects the waste heat back into the feedwater ahead of the heaters. This concept has boosted the generator output by almost 5 MWe and reduced the capacity of the condensate and size requirements for both the high- and low-pressure heater areas. The overall design of figure 7 has made optimal use of these improvements to maximize plant output and reduce cost.

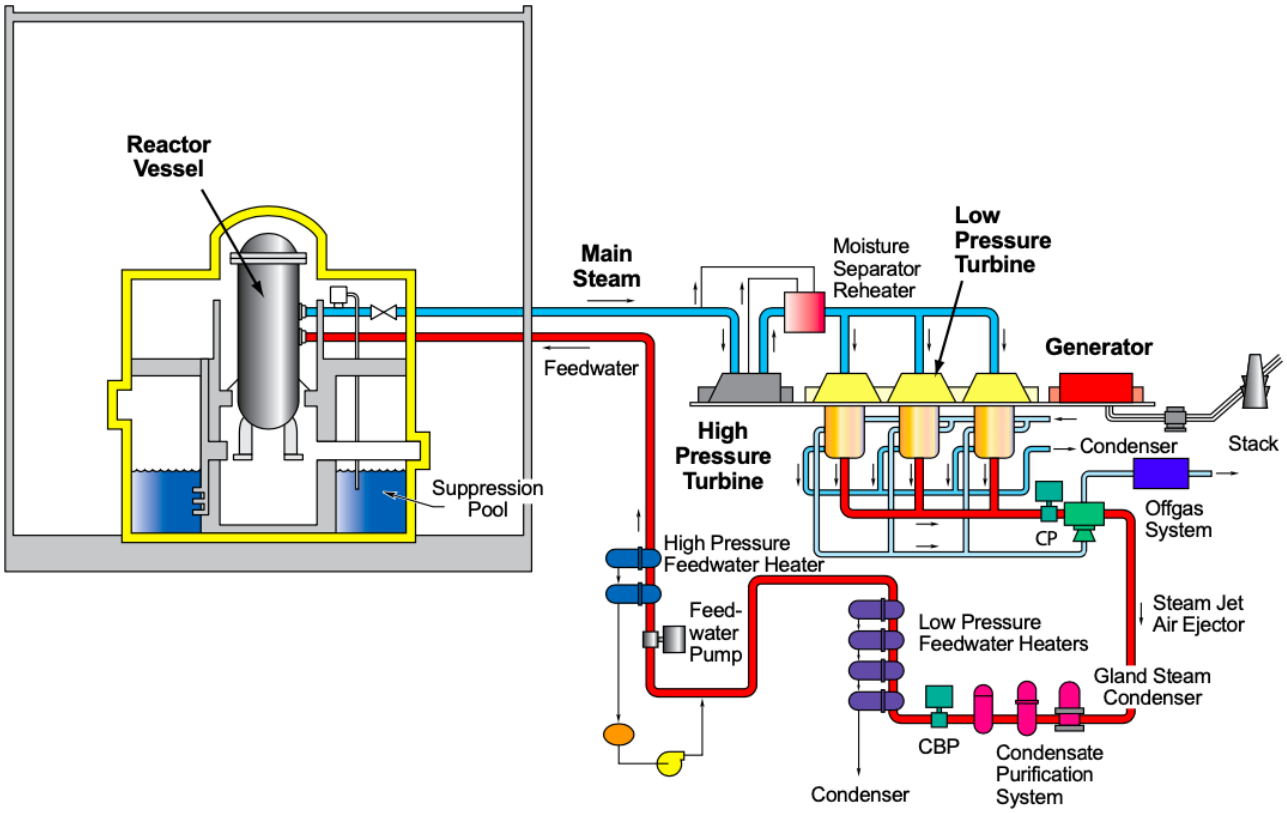

Figure 7: The Steam and Power Conversion System from [1]

The Steam and Power Conversion (S&PC) System is composed of various components that utilize the steam generated by the reactor to produce electrical power of about 1350 MWe. The components of the system include the main turbine generator system, main condenser, condenser evacuation system, turbine bypass system, extraction steam system, condensate cleanup system, and the condensate and feedwater pumping and heating system. Heat rejected to the main condenser is eliminated by a circulating water system that discharges it to the power cycle heat sink.

Steam produced in the reactor is delivered to the high-pressure turbine and reheaters. It then moves through a combined moisture separator/reheater before entering the low-pressure turbines. The heater drain pumps return the moisture separator drains, steam reheater drains, and the drains from the two high-pressure feedwater heaters to the reactor feedwater pump section. The drains pass first through the high-pressure feedwater heaters before feeding the reactor. The low-pressure feedwater heater drains are sent to the condenser. The steam exhausted from the low-pressure turbines is condensed and deaerated in the condenser. The condensate boost pumps deliver the feedwater through the low-pressure feedwater heaters to the reactor feed pumps.

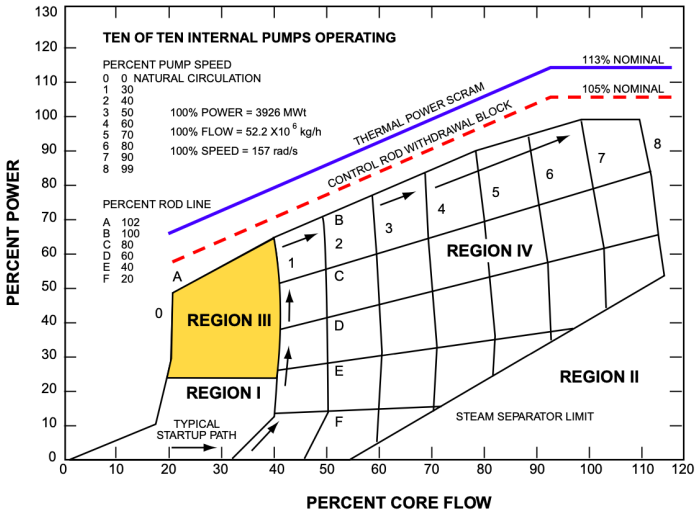

Figure 8: ABWR Power Flow map from [1].

3 Operational principles of the power plant

The operation of the BWR is relatively simple during normal conditions, owing to the direct cycle's strong interdependence between the reactor's thermal power, pressure, and water level. These parameters are closely connected, which allows for their automated control. To modify the thermal power and steam flow rate, the re-circulation flow rate or control rod position can be adjusted. The steam dome pressure in the reactor pressure vessel is maintained automatically at a constant value by regulating the opening of the main turbine control valves or, in the event of a significant pressure increase, by opening the turbine valves to send some of the steam directly to the main condenser. The reactor water level is also automatically maintained at a constant level by controlling the speed of the reactor water feed pumps and, hence, the feedwater flow rate. Automatic load following above 65% power is accomplished by changing only the re-circulation flow. Below this level, control rods are used to regulate the power.

3.1 Startup and shudown of the reactor

The ABWR offers simple startup and shutdown procedures. During plant startup, the reactor is brought to criticality by withdrawing control rods. The Reactor vessel is then heated and pressurized while increasing reactor power by further withdrawing control rods. The reactor power is gradually increased until certain conditions are met, such as synchronization of the main turbine, application of the first load to the generator, and reaching the automatic re-circulation flow control range. Once the last condition is reached, reactor power is increased by increasing the re-circulation flow rate.

At full power operation, the turbine operates in a "turbine-follow-reactor" mode, accepting the steam generated by the reactor. During plant shutdown, the procedure is reversed. After the control rods are fully inserted, the reactor is cooled down and decay heat is removed by diverting steam to the main condenser and operating the Residual Heat Removal System.

The ABWR operating map (see figure 8) shows the steady-state relationship between reactor power and re-circulation flow. Control rod lines, which represent prescribed control rod patterns, are nearly horizontal, while lines of constant re-circulation pump speeds are nearly vertical. Any operational path that changes the power and flow from one condition to another can be traced on this map through control rod maneuver or re-circulation flow change.

However, certain areas of the map are off-limits for various reasons. For example, some regions may be prohibited to maintain core thermal limits, prevent core instability, avoid operation above the licensed power level, or prevent excess moisture in the steam from reaching the main turbine.

Despite the numerous possibilities shown on the power-flow map, normal plant operation typically occurs along the 100% control rod line. The power-flow map also illustrates the trajectory for normal plant startup and shutdown, with automatic protective interlocks in place to prevent any operation outside of prescribed limits or to initiate an automatic reactor shutdown if necessary.

3.2 Automatic load-following operation

The ABWR is capable of meeting grid requirements for frequency control, load regulation, and load following. operating in the "turbine-follow-reactor", the reactor is able to respond quickly and automatically to changes in turbine/load demand by using of automatic process

control systems. This ensures that the generated steam flow matches the required flow rate for the turbine to maintain proper load and frequency operation.

The ABWR is capable of changing power output at a rate of approximately 1% per second using only re-circulation flow changes in the 65% to 100% power range. Below 65% power, power change rate is approximately 2.5% per minute using control rod motion. These capabilities are significantly faster than what is required to respond to load and frequency changes, which ensures stable and reliable operation of the power plant.

3.3 Improvement to operation and maintenance

To simplify the operation and maintenance burden for utilities, the design of every electrical and mechanical system in the ABWR power plant has been focused on improved operation and maintenance.

In a ABWR the control rod are equipped of the The Fine motion control rod drives which replaces the external beam supports of the current BWRs. The Fine motion control rod drives simplify operation and maintenance tasks, reduce radiation exposure, and improve maintainability. They use electric fine rod motion during normal operation and hydraulic pressure for scram insertion. In addition, they incorporate integral shootout steel that replaces external beam supports and allow for control rods to be moved in small increments, reducing core thermal power and fuel stress. This fine motion capability improves fuel rod integrity, burn rate reactivity compensation and operability, even at high power levels. Furthermore, simultaneous operation of multiple control rods shortens plant startup time and increases availability.

Moreover, the use of digital technologies with automated, self-diagnostic features, and fiber optic cable has simplified controls and instrumentation, while reducing cabling.

Improvements have been made to the Neutron Monitoring System, with fixed wide range neutron detectors replacing retractable source and intermediate range monitors. The man-machine interface has been simplified using advanced technologies such as large, flat-panel displays, touch-screen, and function-oriented keyboards. The ABWR design features increased system redundancies, permitting on-line maintenance, and significantly reducing forced and planned maintenance outages.

4 Safety features of the power plant

The ABWR is equiped with a number of safety systems designed to respond to the following events: operational transients, design basis accidents, special regulatory mandated events and beyond design basis accidents. The use of reactor internal pumps allows the elimination of external recirculation loops connected to the Reactor Pressure Vessel (RPV) below the top of the core region, which allows for a reduced capacity Emergency Core Cooling System, for the same efficiency. Those systems allow for a Core Damage Frequency (CDF) as low as 1.6×10^{-7} per year.

4.1 Emergency Core Cooling Systems

The Emergency Core Cooling Systems (ECCS) consist in three independent and redundant divisions, each of them comprising a high pressure and low pressure coolant makeup system. They are designed to remove residual heat from the reactor in case the normal cooling system has failed.

4.1.1 High Pressure Core Flooder

The High Pressure Core Flooder system is designed to inject water in the reactor in order to maintain reactor vessel coolant inventory following a small break Loss of Coolant Accident (LOCA) that do not depressurize the reactor. This system is automatically initiated by either a high pressure signal in the drywell or a low water level signal in the RPV. Water can either be injected from the Condensate Storage Tank (CST) or the Suppression Pool (SP), as shown in Fig. 9.

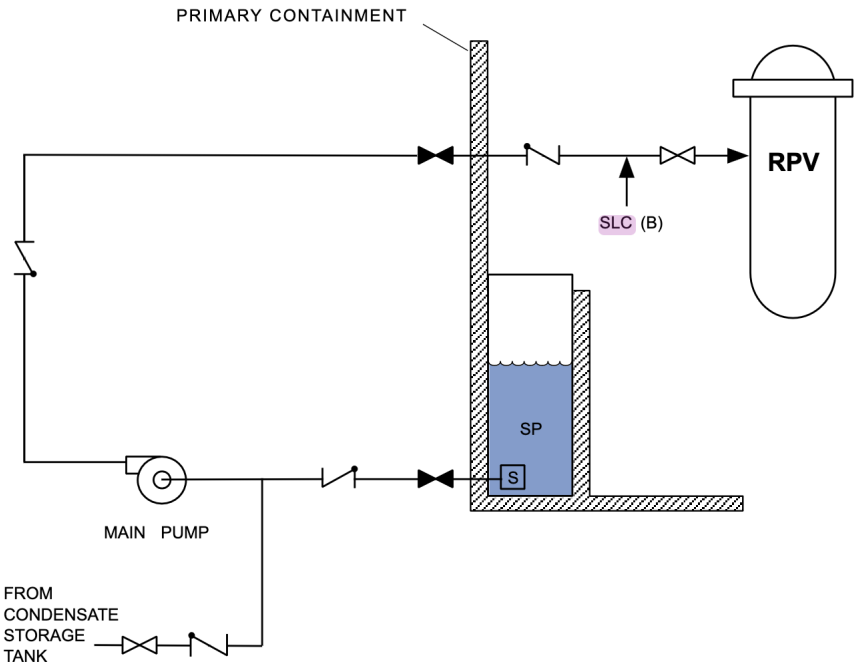

Figure 9: Diagram of the HPCF system, from [1].

4.1.2 Reactor Core Isolation Cooling

The Reactor Core Isolation Cooling system (RCIC) is designed to provide cooling water to the reactor when the vessel is isolated (i.e the steam is not flowing to the main turbine and through the main condenser). It also replaces and act like a HPCF system on one of the three ECCS division. The RCIC uses a steam-driven turbine pump to maintain sufficient water level in the RPV and will start automatically for the following events:

- the vessel is isolated and maintained in hot standby,
- loss of normal feedwater before the reactor is depressurized to a level where the shutdown cooling system can be placed in operation,

- complete loss of AC power.

The water supply for the RCIC is either the CST or the SP, with coolant flow discharged in one of the main feedwater line. The steam-driven turbine exhaust in the SP, as shown in Fig. 10.

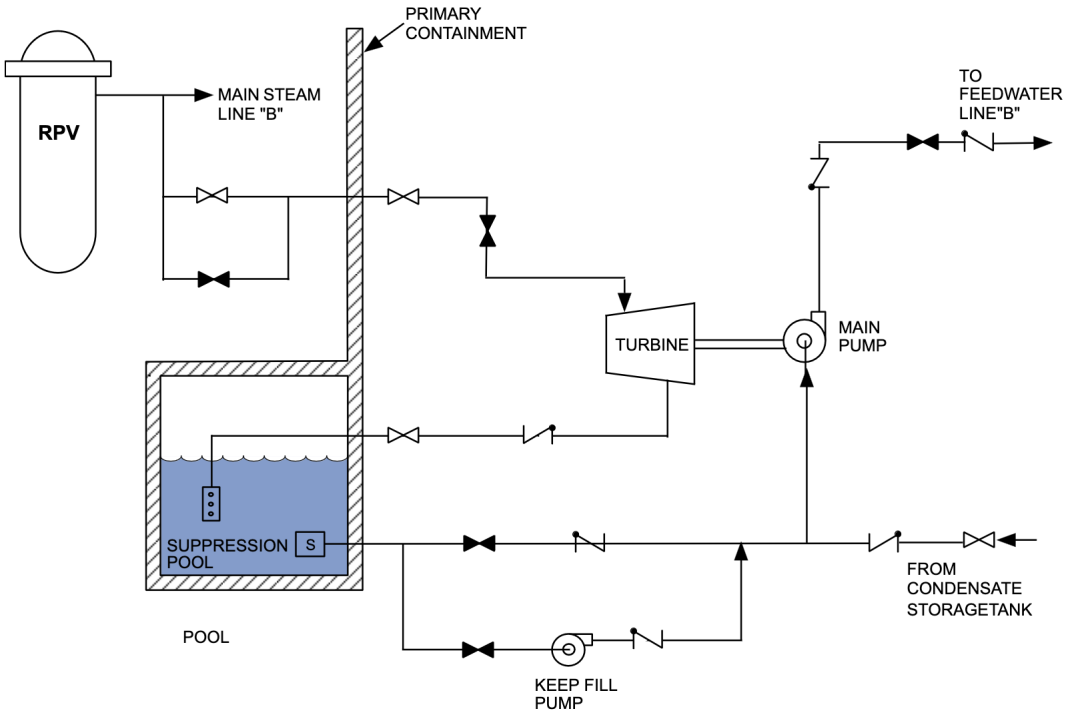

Figure 10: Diagram of the RCIC system, from [1].

4.1.3 Residual Heat Removal

The Residual Heat Removal system (RHR) is designed to remove residual heat from the reactor during shutdown, isolation and LOCA. This system has six principal functions:

- Low Pressure Flooder (LPFL): this system is divided in three loops and is designed to inject water in the reactor following its depressurization.
- Suppression Pool Water Cooling (SPC): this system is designed to cool the suppression pool water below 49°C during normal operation by using the RHR heat exchangers.
- Reactor Shutdown Cooling (SDC): this system removes decay heat from the reactor after shutdown.
- Primary Containment Vessel Spray Cooling: this system is designed to spray water from the SP in the drywell following a LOCA, in order to keep the pressure and temperature of the primary containment within the designated range.
- Supplemental Fuel Pool Cooling (FPC): this system removes heat from the fuel pool during shutdown in case the designated fuel pool cooling system is unable to maintain the pool water temperature below the required limit.
- AC-Independent Water Addition (ACIWA): this system provides a way to inject water from the fire protection system in the RPV, drywell or wetwell in case of the loss of AC power.

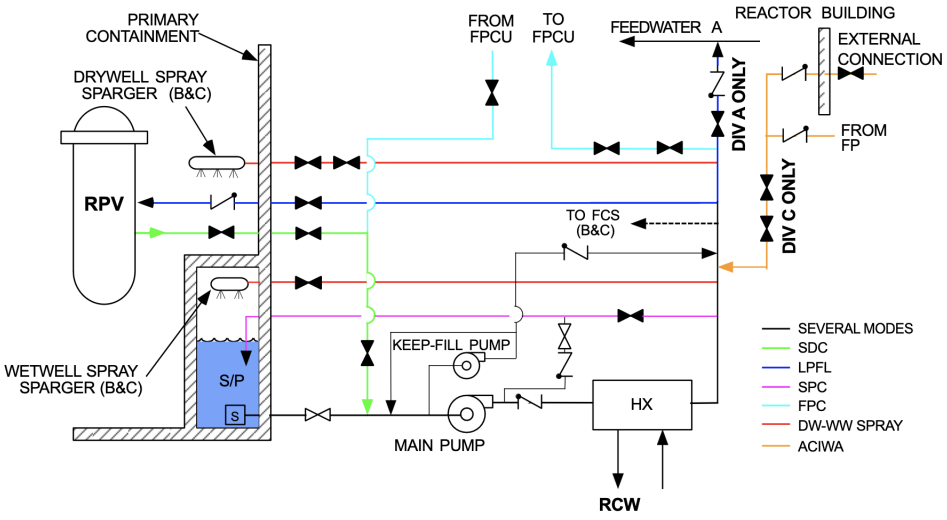

Figure 11: Diagram of the RHR system, from [1].

4.1.4 Automatic Depressurization System

The Automatic Depressurization System (ADS) directs steam passing through the main steam line to the suppression pools when it receives a signal for low water level in the reactor pressure vessel and high pressure in the dry-well. It is activated with a delay to allow the HPCF a chance to restore the water level in the RPV.

4.2 Other Safety Systems

4.2.1 Standby Gas Treatment System (SGTS)

This system is designed to treat and discharge primary or secondary containment air to the plant stack. In case of LOCA, it maintains a negative pressure inside the secondary containment to avoid the release of radioactive gases in the environment.

4.2.2 Atmospheric Control System (ACS)

This system establishes an inert atmosphere (nitrogen) inside the primary containement to greatly decrease the oxygen concentration and thus reduce the risk of fire in case hydrogen is released.

4.2.3 Flammability Control System

This system is made of thermal hydrogen and oxygen recombinators designed to maintain oxygen concentration below the flammability limit by recombining hydrogen and oxygen without relying on purging or releasing radioactive material to the environment.

4.2.4 Standby Liquid Control System (SLCS

This system is a backup method to bring the nuclear reactor to subcriticality and to maintain subcriticality as the reactor cools. It allows the injection of a sodium pentaborate solution in the core to absorb thermal neutrons and kill the chain reaction.

4.2.5 Emergency Diesel Generator (EDG)

They provide power to the safety systems when offsite power is lost.

5 Calculation of selected core parameters

The purpose of this task is to calculate the following core-average thermal-hydraulics characteristics of the reactor:

- the axial pressure drop,
- the axial coolant enthalpy distribution,
- the axial void fraction distribution
- the axial coolant temperature distribution
- the flow characteristic of the core, i.e the pressure drop as a function of mass flux for different percentages of nominal core power.

5.1 Theory

In order to obtain the axial distribution of the parameters cited above, we will axially divide a channel into cells and calculate the thermal-hydraulics properties in each cell. We will use the whole assembly model for the calculations in the channel. The power is first defined by assigning the total power to each fuel rod:

$$q_{av} = \frac{Q_{tot}}{N_{fr} N_{fa}}, \tag{1}$$

where Q_tot is the total thermal power of the core, N_{fr} and N_{fa} are the number of fuel rods per assembly and number of fuel assemblies, respectively. Then, the typical cosine distribution for cylindrical core is applied, with the axial peaking factor taken into account, and the power is normalized by the number of cells:

$$q_{cell} = \frac{q_{av}}{N_{cell}} f_z \cos\left(\frac{\pi z}{H_e}\right), \tag{2}$$

where N_{cell} is the number of cells, H_e is the extrapolated length and f_z is the axial peaking factor:

$$f_z = \frac{\pi H}{2 H_e \sin\left(\frac{\pi}{2}\frac{H}{H_e}\right)}, \tag{3}$$

where $\frac{H}{H_e} = \frac{5}{6}$. The enthalpy in cell k is calculated as:

$$i(k) = i(k-1) + \frac{(q_{cell}(k-1) + q_{cell}(k)) P_H}{2W}, \tag{4}$$

where P_H is the heated perimeter and W is the mass flow in the channel.

The pressure drop and void fraction calculations are carried out using the HEM model. The total pressure drop in a cell is the sum of the gravity, acceleration, friction and local pressure drops:

$$-\Delta p = r_3 C_f \frac{4L}{D}\frac{G^2}{2\rho_f} + r_4 L \rho_f g + r_2 \frac{G^2}{\rho_f} + \left(\sum_{i=1}^{N} \Phi_{lo,i}^2 \xi_i\right)\frac{G^2}{2\rho_f}, \tag{5}$$

where:

- C_f is the friction coefficient, calculated with the Haaland formula,
- L is the length of the cell,
- D is the hydraulic diameter of the cell,
- G is the mass flux in the channel,
- ρ_f is the saturated liquid density,
- ρ_g is the saturated vapor density,
- g is the standard gravity,
- $\Phi_{lo,i}^2$ is the local loss multiplier,

- ξ_i is the local loss coefficient,
- r_3 is the friction multiplier: $r_3 = \frac{1}{L}\int_0^L \Phi_{lo}^2 dz$,
- r_4 is the gravity multiplier: $r_4 = \frac{1}{L\rho_f}\int_0^L [\alpha\rho_g + (1-\alpha)\rho_f]dz$,
- r_2 is the acceleration multiplier: $r_2 = \rho_f \int_0^L \frac{d}{dz}[\frac{x^2}{\alpha\rho_g} + \frac{(1-x)^2}{(1-\alpha)\rho_f}]dz$,
- x is the equilibrium quality,
- α is the void fraction.

The equilibrium quality is calculated by using the enthalpy:

$$x(k) = \frac{i(k) - i_l(k)}{i_g(k) - i_l(k)}, \tag{6}$$

where $i_g(k)$ and $i_l(k)$ are the saturated vapor and liquid enthalpies, respectively. The void fraction is calculated as a function of the equilibrium quality:

$$\alpha = \frac{1}{1 + \frac{\rho_g}{\rho_f}\left(\frac{1-x}{x}\right)} \tag{7}$$

Once the pressure distribution is known in the channel, the temperature is calculated as a function of enthalpy and pressure, using XSteam tables [4].

5.2 Results

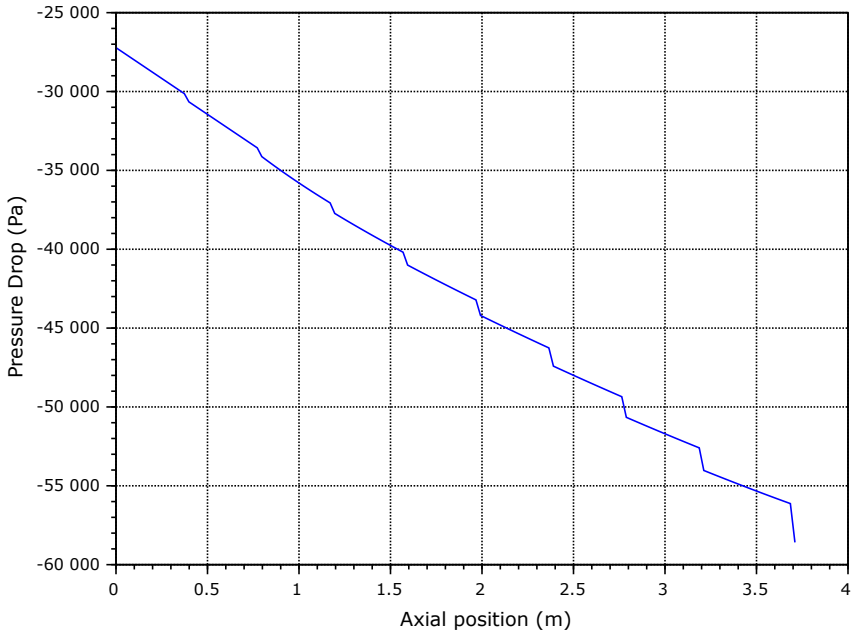

Figure 12: Pressure drop as a function of channel height.

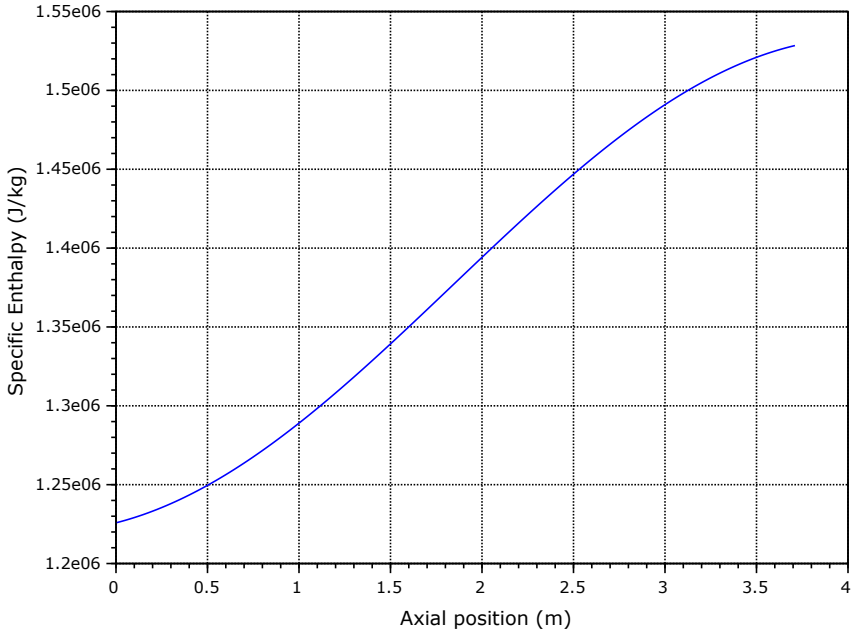

Figure 13: Enthalpy distribution as a function of channel height.

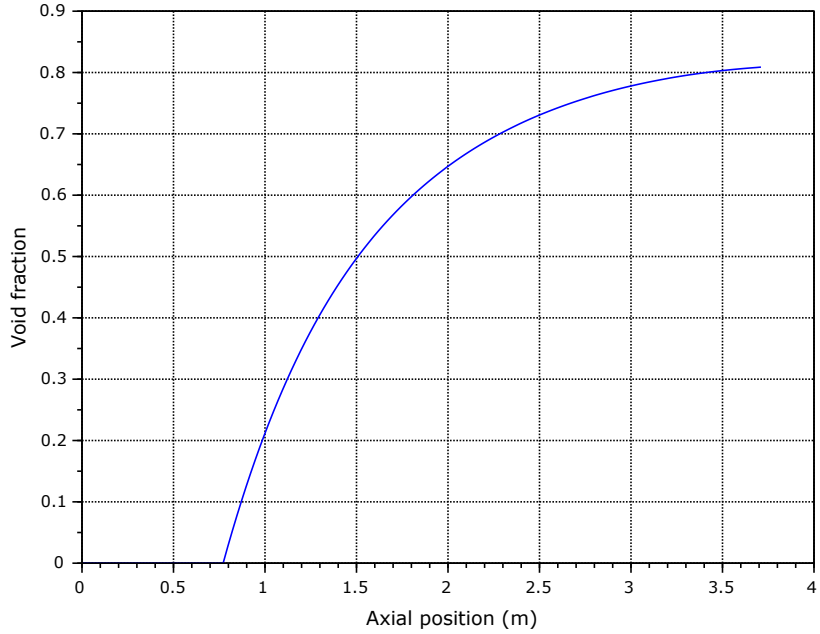

Figure 14: Void fraction distribution as a function of channel height.

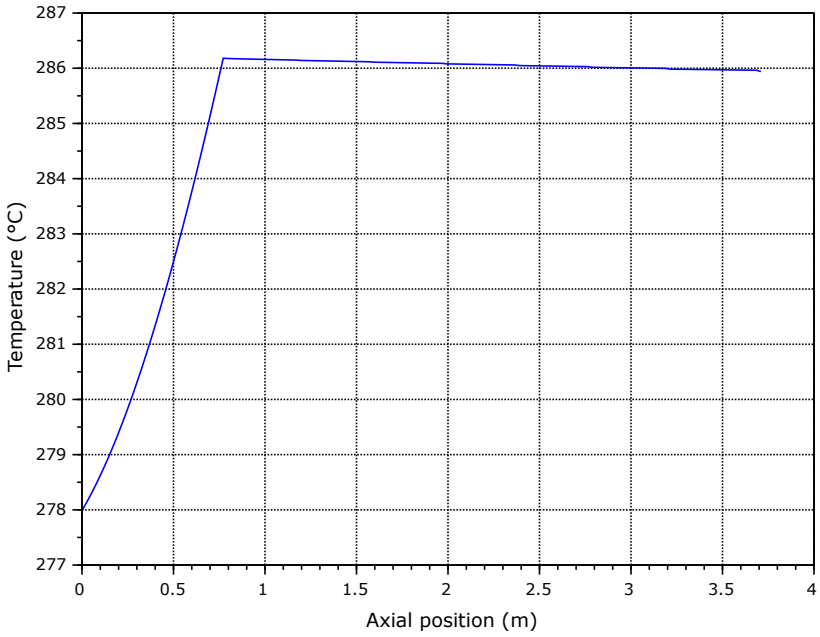

Figure 15: Coolant temperature distribution in the channel.

We see on Fig. 15 that upon reaching the saturation point, the coolant temperature slightly decreases. This is due to the fact that the pressure in the channel also decreases, thus lowering the saturation point and the saturation temperature.

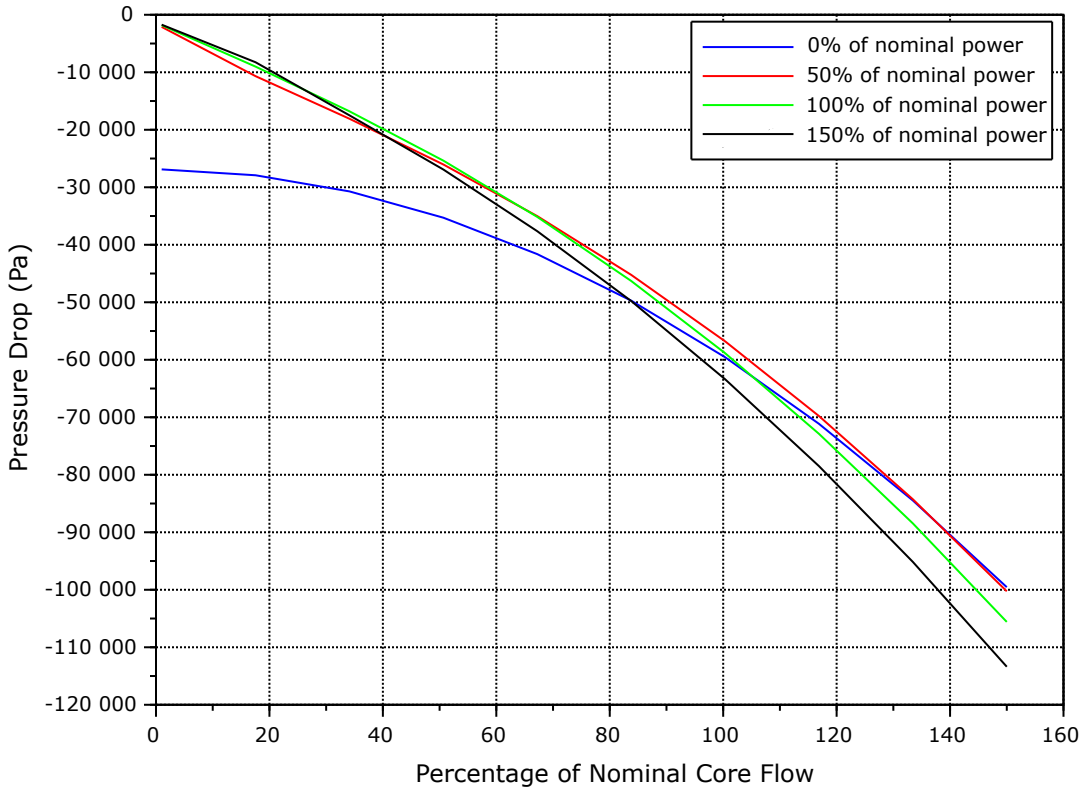

Figure 16: Flow characteristic of the core.

6 Calculations of CHF margins in a hot channel

The aim of this task is to calculate the minimum critical power ratio (MCPR) of the core, which is the ratio of the critical power, the power at which dryout occurs in a channel, to the actual power in this channel. Dryout occurs when the thin liquid film directly in contact with the surface of fuel rods starts to evaporate and disappear, thus greatly decreasing the heat transfer between fuel and coolant and increasing the risk of core damage.

6.1 Theory

We will calculate CPR in a hot channel, as it is where the dryout is most likely to develop first. The power of the hot channel is found by multiplying the average channel power of Eq. 2 by the radial peaking factor, f_r:

$$f_r = \frac{2.405R}{2R_e J_1\left(\frac{2.405R}{R_e}\right)}, \tag{8}$$

where $\frac{R}{R_e} = \frac{5}{6}$.

The critical power ratio is given by:

$$CPR = \frac{q_{cr}}{q_a} = \frac{x_{cr} - x_{in}}{x_{ex} - x_{in}}, \tag{9}$$

where q_{cr} is the critical power, q_a is the actual power in the channel, x_{cr} is the critical quality, x_{in} is the inlet quality and x_{ex} is the exit quality. The critical quality is calculated with the GE-CISE correlation

$$x_{cr} = 1.24\frac{A * L_B^*}{B + L_B^*}, \tag{10}$$

where:

- $L_B^* = L_B/0.0254$, L_B is the boiling length to dryout,
- $A = 1.055 - 0.013\left(\frac{p_R - 600}{400}\right)^2 - 1.233G_R + 0.907G_R^2 - 0.285G_R^3$
- $B = 17.98 + 78.873G_R - 35.464G_R^2$
- $G_R = G/1356.23$, G is the mass flux in kg/m^2.s
- $p_R = p/6894.757$, p is the pressure in Pa.

6.2 Results

In the hot channel, we found:

$$MCPR = 1.10 \tag{11}$$

which means dryout is not occurring in the core, with a 10% margin in power relative to the power in the hot channel. Fig. 17 shows the comparison of different thermo-hydraulics parameters between average and hot channel.

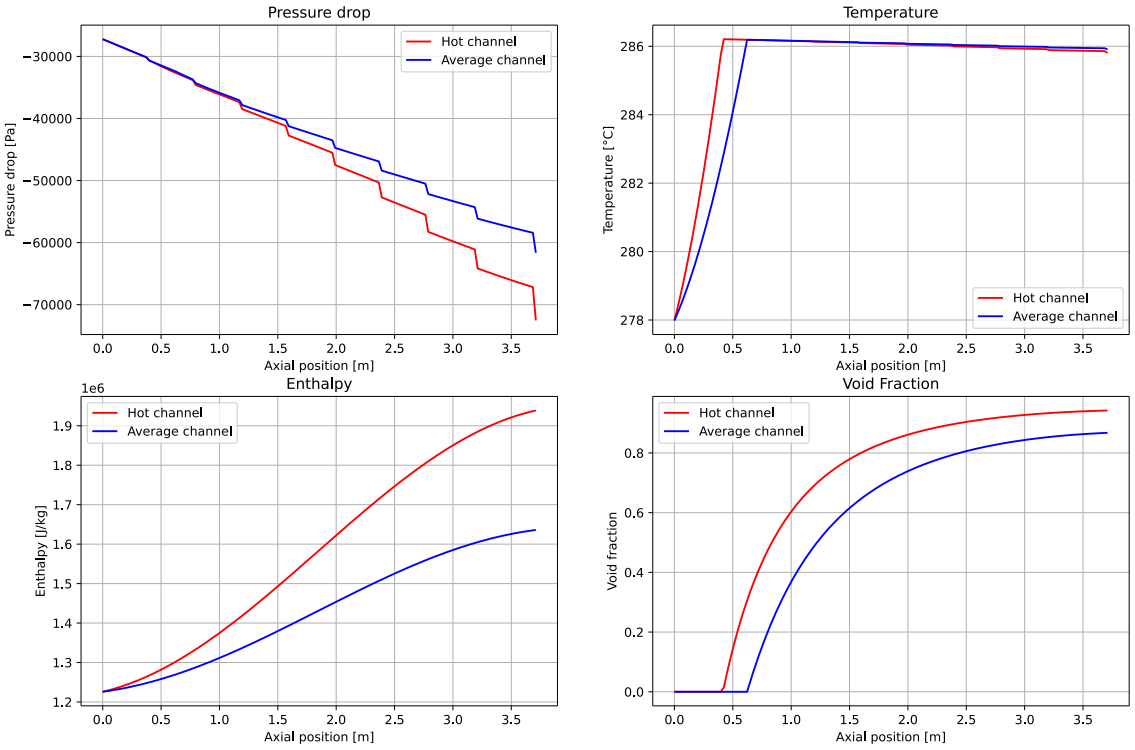

Figure 17: Thermo-hydraulics characteristics of the average and hot channels.

7 Calculation of the maximum cladding and fuel pellet temperature

This task aims to identify and calculate the maximum fuel and cladding temperatures of a nuclear reactor. This is necessary for ensuring the safe operation of the reactor since the fuel temperature must not exceed the melting temperature of the fuel material at any point, and the clad temperature should be kept below the maximum allowed value to avoid the hydrogen release. In order to accurately calculate these temperatures, realistic material properties of the clad and fuel are taken into account, as well as temperature-dependent thermal conductivity of the clad and fuel materials.

7.1 System Presentation

Consider a fuel rod with a diameter of 10.4 mm surrounded by a clad with a inner diameter of 11.46 mm and outer of 12.26 mm, and separated from it by a gap filled with helium. Let T_{Fc} denote the temperature at the center of the fuel, T_{Fo} the outlet temperature of the fuel, T_{Go} the outlet temperature of the gap, and T_{Co} the outlet temperature of the clad. Given only the coolant temperature T_{lb} and the thermal power emitted by the reactor, we need to determine the temperature distribution at the center of the fuel.

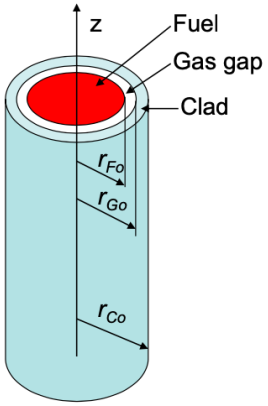

Figure 18: Scheme of the fuel Pellet

To determine the temperature required, we need to calculate the heat generated by a fuel rod. The total thermal power of our reactor is $Q_{tot} = 0.95 \times 3926\ MW$. We assign 94.5% of this total power to fuel pellets. The average power density (source term) in fuel pellets can be calculated using the following equation:

$$q'''av = \frac{Qtot}{N_{FA}\, N_{FR}\, V_{fuel}} \tag{12}$$

Here, N_{FA} represents the number of fuel assemblies, N_{FR} denotes the number of fuel rods in a fuel assembly, and V_{fuel} is the volume of a fuel rod.

Next, we can calculate the power density distribution in a fuel pellet using the following equation:

$$q'''av(z) = q'''av f_R f_A \cos\left(\frac{\pi z}{H_e}\right) \tag{13}$$

where, f_R and f_A are the radial and axial peaking factors, and H_e represents the extrapolated distance. The power density distribution is shown in figure 19

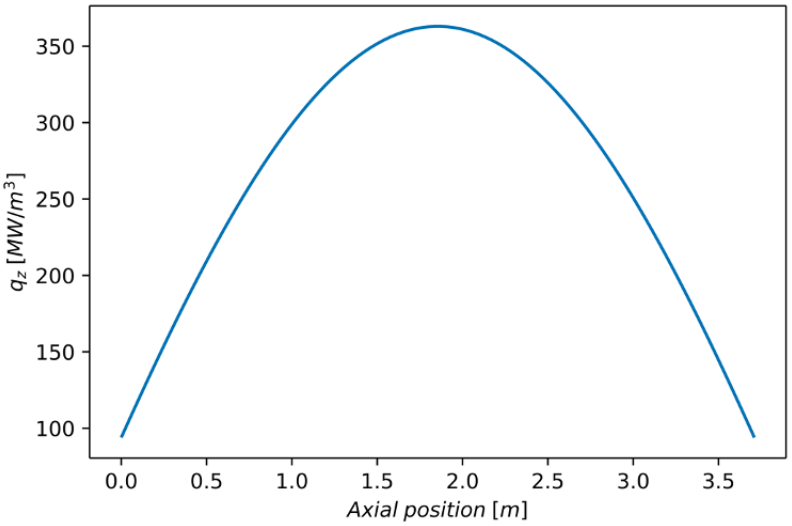

Figure 19: Power density distribution in a pellet.

7.2 Heat equation

From the temperature of the flow we can go back to the one in the center of the fuel with the heat equation in each region :

- Fuel

$$\frac{1}{r}\frac{\partial}{\partial r}\left(r\lambda_F(T)\frac{\partial T}{\partial r}\right) = -q'''(z) \tag{14}$$

- Gas gap

$$\frac{1}{r}\frac{\partial}{\partial r}\left(r\lambda_G\frac{\partial T}{\partial r}\right) = 0 \tag{15}$$

- Clad

$$\frac{1}{r}\frac{\partial}{\partial r}\left(r\lambda_C(T)\frac{\partial T}{\partial r}\right) = 0 \tag{16}$$

where T represents temperature, λ represents conductivity, and r represents radial distance. The term $q'''(z)$ is the source term calculated in equation 13.

The thermal conductivity of the fuel and clad varies with temperature. For solid UO_2 with 95% density, we can use the recommended thermal conductivity equation:

$$\lambda_F(T) = \frac{100}{7.5408 + 17.692t + 3.6142t^2} + \frac{6400}{t^{5/2}}exp(-\frac{16.35}{t}), \tag{17}$$

where $t = T/1000$ and T is the temperature in Kelvin.

For the temperature-dependent conductivity of the clad, we can use:

$$\lambda_C(T) = 12.6 + 0.0118T, \tag{18}$$

where T in temperature in degree The gas gap conductivity is fixed at $0.3Wm^{-1}K^{-1}$.

7.3 Resolution of the equation

7.3.1 Caculation of T_{CO}

From coolant temperature T_{lb} we can deduce the outer temperature of the clad T_{CO} with the thermal boundary layer in coolant which follow the Newton equation for the convective heat transfer:

$$q''|_{rCO} = h(T_{lb} - T_{OC}) \tag{19}$$

where h is the heat transfer coefficient.

Since $q''|_{rCO}2\pi r_{CO}dz = q'''\pi r_{FO}^2 dz$ we have $q''|_{rCO} = \frac{q'''r_{FO}^2}{2r_{CO}}$. Thus we obtain the equation

$$T_{Co} = \frac{q'''r_{FO}^2}{2r_{CO}h} + T_{lb} \tag{20}$$

The Chen relation is used to estimate the heat transfer coefficient h for two-phase flow in a tube. The principle to find the suitable h is presented in figure 20. It is based on the concept of two-phase heat transfer coefficient, which is the product of the single-phase heat transfer coefficient and the two-phase multiplier. The two-phase multiplier is a factor that accounts for the enhancement of heat transfer due to the presence of the two phases.

7.3.2 Calculation of T_{GO}

Integrating Equation 16 over the radial distance r, we obtain:

$$q''\Big|_{r_{GO}} = \lambda_C(T)\frac{dT_G}{dr}\Big|_{r_{GO}} = -\frac{C'}{r}. \tag{21}$$

Using the relation $q''|rGO2\pi r_{GO}dz = q'''\pi r_{FO}^2 dz$, we can deduce that $C' = -\frac{q'''r_{FO}^2}{2}$.

Since the fuel conductivity is temperature-dependent, the second integration in Equation 22 must be performed as follows:

$$\int_{T_{GO}}^{T_{CO}} \lambda_G(T)dT = \int_0^{rCO} -\frac{C''}{r}dr. \tag{22}$$

The second term of Equation 22 can be easily calculated, which yields a function of T_{GO} that is equal to a constant. We can solve this equation using the dichotomy method, which gives us the value of T_{GO}.

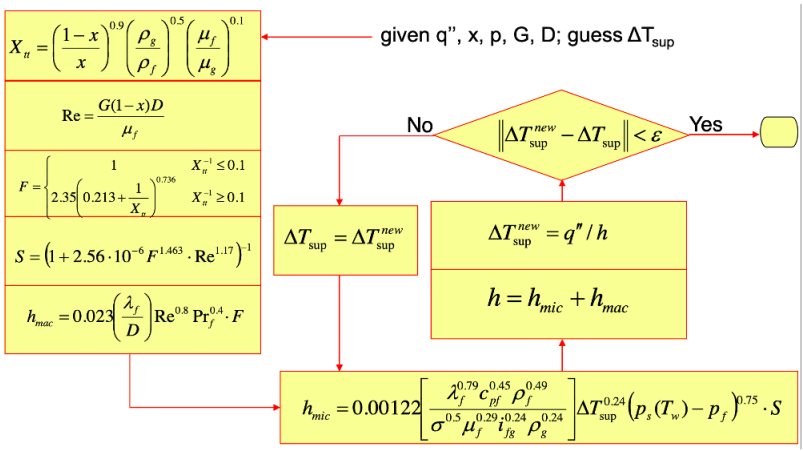

Figure 20: Presentation of the Chen correlation.

7.3.3 Calculation of T_{FO}

The heat equation for the gap region is given by Equation 15. Although this equation is the same as the one for the clad region, we assume that the thermal conductivity is constant. As a result, we can analytically calculate T_{FO} by integrating Equation 15 twice over r:

$$\lambda_G \frac{dT_G}{dr}\bigg|_{r_{FO}} = -\frac{C'}{r} \rightarrow T_G(r) = \frac{C'}{\lambda_G}\ln(r) + C'' \tag{23}$$

Here, $C' = \frac{q'''r_{FO}^2}{2}$ and $C'' = T_{FO}$ are constants that can be determined using boundary conditions, as in the previous section. Thus, we obtain the following expression for T_{FO}:

$$T_{FO} = T_{GO} + \frac{q'''r_{FO}^2}{2\lambda_G}\ln\left(\frac{r_{GO}}{r_{FO}}\right) \tag{24}$$

7.3.4 Calculation of T_{FC}

The heat equation for the fuel region is given by Equation 14. Integrating this equation from 0 to r_{FO} yields:

$$\lambda_F(T)\frac{dT_F}{dr}\bigg|_{r_{FO}} = -\frac{1}{r}\int_0^{r_{FO}} q'''(z)rdr = -\frac{q'''(z)r}{2} + \frac{C}{r} \tag{25}$$

To ensure that the temperature at the center of the fuel pellet, denoted by T_{FC}, is limited, the constant C must be equal to zero, i.e., $C = 0$. Consequently, we obtain:

$$\lambda_F(T)\frac{dT_F}{dr}\bigg|_{r_{GO}} = -\frac{q'''(z)r}{2} \tag{26}$$

Once again, this equation involves a first term that is a function of T_{FC}, while the second term is computable. Solving this equation for T_{FC} can be done using a dichotomy method.

7.4 Results

Figures 21 and 22 show the axial temperature distributions for the fuel pellet and the clad, respectively. Specifically, Figure 21 displays the temperature at the center of the fuel pellet, denoted by T_{FC}, while Figure 22 shows the temperature in the clad, denoted by T_C.

7.5 Discussion

The maximum fuel and clad temperatures in an Advanced Boiling Water Reactor (ABWR) depend on various operating and design conditions. However, some typical values can be provided based on design specifications and analyses.

The maximum temperature of the fuel pellets in an ABWR is typically around 2600°C. The fuel pellets are made of uranium dioxide (UO2), which has a high melting point and can withstand such high temperatures without melting. However, the fuel pellets can experience thermal stresses and cracking at such high temperatures, which can affect their performance and integrity.

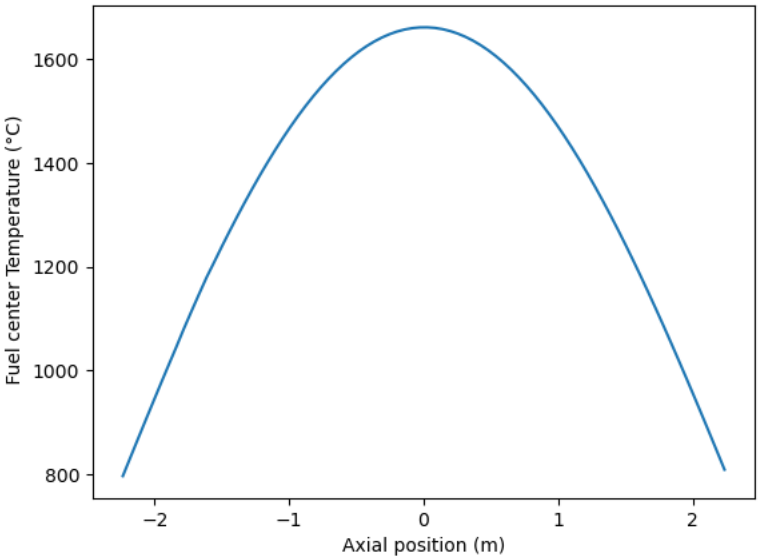

Figure 21: Axial temperature distributions for the fuel pellet.

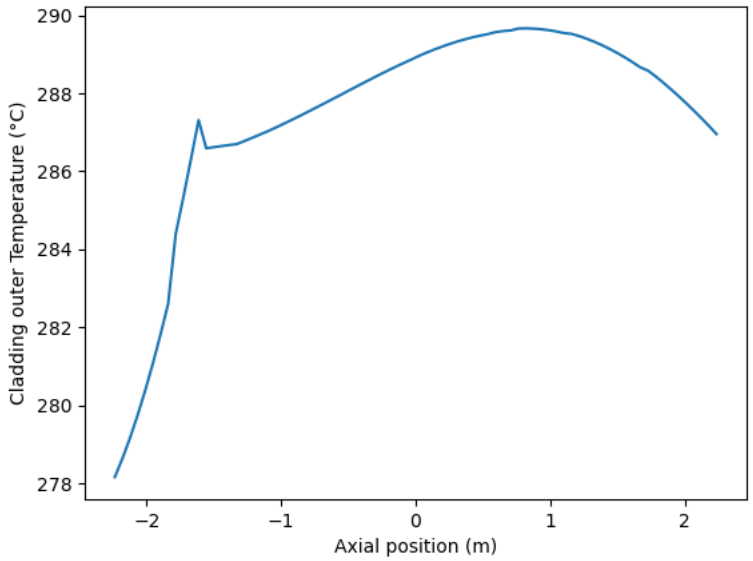

Figure 22: Axial temperature distributions for the clad.

The maximum temperature of the clad in an ABWR is typically around 1200°C. The clad is made of a zirconium alloy, which has a lower melting point than UO2 and is more susceptible to deformation and failure at high temperatures. Therefore, the maximum temperature of the clad is usually limited to around 1200°C to ensure its integrity and prevent accidents.

The temperatures we get in figure 21 and 22 show that we are below the limits as expected.

References

[1] GE_Hitachi, *Abwr general description book*, 2007.

[2] A. Prieto-Guerrero and G. Espinosa-Paredes, "Description of boiling water reactors," in *Linear and Non-Linear Stability Analysis in Boiling Water Reactors*, ser. Woodhead Publishing Series in Energy, A. Prieto-Guerrero and G. Espinosa-Paredes, Eds., Woodhead Publishing, 2019, pp. 25–55, ISBN: 978-0-08-102445-4. DOI: https://doi.org/10.1016/B978-0-08-102445-4.00002-3. [Online]. Available: https://www.sciencedirect.com/science/article/pii/B9780081024454000023.

[3] "Abwr design control document, chapter 4 : Reactor," GE Nuclear Energy, Tech. Rep., 1997. [Online]. Available: https://www.nrc.gov/docs/ML1112/ML11126A104.pdf.

[4] M. Holmgren, *Xsteam, thermodynamic properties of water and steam*, 2023. [Online]. Available: https://xsteam.sourceforge.net/.